

Desalination of Polymer-Flooding Produced Water at Increased Water Recovery and Minimized Energy

Industrial & Engineering Chemistry Research

Sosa-Fernandez, Paulina A.; Post, Jan W.; Karemore, Apurva; Bruning, Harry; Rijnaarts, Huub H.M.

<https://doi.org/10.1021/acs.iecr.0c02088>

This publication is made publicly available in the institutional repository of Wageningen University and Research, under the terms of article 25fa of the Dutch Copyright Act, also known as the Amendment Taverne. This has been done with explicit consent by the author.

Article 25fa states that the author of a short scientific work funded either wholly or partially by Dutch public funds is entitled to make that work publicly available for no consideration following a reasonable period of time after the work was first published, provided that clear reference is made to the source of the first publication of the work.

This publication is distributed under The Association of Universities in the Netherlands (VSNU) 'Article 25fa implementation' project. In this project research outputs of researchers employed by Dutch Universities that comply with the legal requirements of Article 25fa of the Dutch Copyright Act are distributed online and free of cost or other barriers in institutional repositories. Research outputs are distributed six months after their first online publication in the original published version and with proper attribution to the source of the original publication.

You are permitted to download and use the publication for personal purposes. All rights remain with the author(s) and / or copyright owner(s) of this work. Any use of the publication or parts of it other than authorised under article 25fa of the Dutch Copyright act is prohibited. Wageningen University & Research and the author(s) of this publication shall not be held responsible or liable for any damages resulting from your (re)use of this publication.

For questions regarding the public availability of this publication please contact openscience.library@wur.nl

Desalination of Polymer-Flooding Produced Water at Increased Water Recovery and Minimized Energy

Paulina A. Sosa-Fernandez,* Jan W. Post,* Apurva Karemore, Harry Bruning, and Huub H. M. Rijnaarts

Cite This: *Ind. Eng. Chem. Res.* 2020, 59, 16059–16067

Read Online

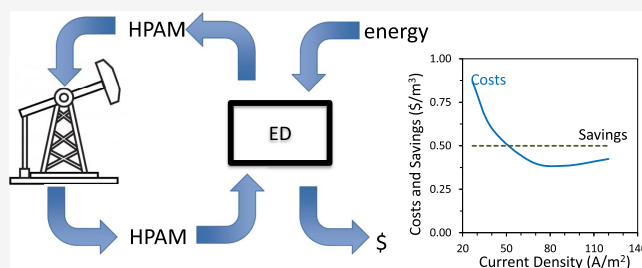
ACCESS |

Metrics & More

Article Recommendations

Supporting Information

ABSTRACT: When desalinating an industrial stream like polymer-flooding produced water via electrodialysis (ED), high water recoveries, low energy consumption, and reduced membrane area are all desirable. However, little effort has been done until now to experimentally achieve these goals. Encouraged by recent and promising results obtained using aliphatic membranes and pulsed electric field, this study experimentally evaluated different strategies and operational conditions to increase the water recovery while keeping a low energy consumption. The results obtained were analyzed to understand the trade-offs in operative time, water recovery, and energy consumption. Finally, the experimental data was employed to perform an economic analysis, which indicated that although further optimization should be possible, current conditions already make ED desalination of polymer-flooding produced water a sound case from an economical point of view.



1. INTRODUCTION

Polymer-flooding produced water (PFPW) is a relatively new waste stream coproduced by the oil and gas industry when polymer-flooding technology is applied to enhance oil recovery from a field. PFPW typically contains varying amounts of dissolved solids, mainly salts, oil, and a viscosifying water-soluble polymer, typically partially hydrolyzed polyacrylamide (HPAM) or one of its derivatives.¹ To be reused in polymer flooding, PFPW should be partially desalinated, a goal that can be achieved by using electrodialysis (ED).^{2,3} However, the mixed composition of PFPW, and particularly the presence of the polyelectrolyte HPAM, makes the desalination by ED challenging due to concentration polarization and fouling.^{1,4,5}

An option to reduce concentration polarization and fouling incidences during ED is to use a pulsed electric field (PEF).⁶ This mode of operation consists of applying the electric current for a short time (pulse), followed by a resting period without current (pause), while the streams are continuously pumped through the ED stack. In this way, the built-up of polarization layers is prevented and fouling can be minimized. In previous investigations, PEF and continuous modes were employed and compared in their performances to desalinate PFPW. Membrane surface analyses revealed that fouling was minimal, with negligible differences between both operation modes. In contrast, noteworthy reductions in energy consumption (above 30%) and increased desalination performance were found, especially when employing a pulse/pause regime of 1 s/1 s.⁷

Although these results were encouraging, the small amount of fouling found on the ion-exchange membranes (IEMs) was a surprise. Two explanations were put forward: either the

duration of the experiments (2–8 h) was too short to accumulate significant amounts of foulants or the membranes employed (FujiFilm type 10) had superior antifouling properties than others previously employed in various studies.^{3,8,9}

Both hypotheses were addressed in a recent study, in which synthetic PFPW was desalinated continuously for 8 days employing stacks composed of different kinds of anion-exchange membranes (AEMs).¹⁰ For similar feed composition and same type of membranes, the desalination performance and membrane analysis indicated more fouling than in the PEF study.⁷ Regarding the role of the membranes, it was found that the likelihood of the stacks reaching the limiting current mainly depended on the resistance of the AEMs. Moreover, the variability in stack desalination performance was larger for aromatic AEMs than for aliphatic AEMs, suggesting that the latter were more adequate to desalinate PFPW.¹⁰

The next step in operationalizing PFPW desalination by advanced ED is to operate the lab-scale system under relevant conditions to optimize energy consumption, capital investment, and water recovery, as well as the trade-offs among these factors, as will be further elaborated.

Received: April 25, 2020
Revised: August 10, 2020
Accepted: August 14, 2020
Published: August 14, 2020



First, the ED process needs to be designed to generate more product and less concentrate, that is, to achieve high water recoveries. After all, the purpose of desalinating PFPW is to reuse it while minimizing the concentrate solution that needs to be further treated or disposed of. However, previous investigations have been conducted at constant water recoveries around 50%. Higher water recoveries could mean less waste, higher energy efficiency, and lower costs.¹¹ With ED, very high water recoveries can be reached, above 90% for some industrial cases.^{12,13} These high recoveries can be achieved by operating the ED in the feed and bleed mode,¹² or in a batch process by splitting the feed disproportionately. Of course, achieving higher water recoveries may also affect energy consumption and likelihood of scaling, both of which could increase.

Another aspect to be considered when designing an electrodialysis process for PFPW is the number of hydraulic stages. Typically, the design values for salt removal in one hydraulic stage are 40–50%, meaning that to increase the amount of salts removed in an ED system, additional stages must be incorporated.¹³ For example, Doornbusch et al. recently found that four stages would be needed to obtain drinking water (Total Dissolved Solids, TDS < 0.5 g/L) from seawater.¹⁴ This is because the operating current density for an electrodialyzer is usually limited by the lowest salinity during the stage. If the process is divided into two or more stages, each stage can be operated at different current densities, which has a positive impact on the production rate but implies more equipment and different energy consumption. In our case study (PFPW mimicking that from the Marmul field in Oman), the salinity of the feed is just below 5.0 g/L,¹⁵ while the desired salinity of the product is around 1.0 g/L,¹⁶ so 80% salt removal is needed. This means that, if PFPW is desalinated in a continuous process, at least two stages would be desirable to achieve the preferred product quality.

Furthermore, there are scarce references in the literature analyzing the cost–benefits of applying PEF at a larger scale. For a nonoptimized system, we achieved energy savings of approximately 30% for a PEF regime of 1 s/1 s.⁷ Because of the pauses during operation, the time required to desalinate a fixed volume of solution was almost doubled. If a production rate is defined, a system operated in PEF with a 1 s/1 s regime would require twice the membrane area needed by an ED system operated in continuous mode. It might be possible to further reduce the pause time and still obtain beneficial results. For example, Mikhaylin et al. found their best results in terms of demineralization rate and low scaling by applying regime pauses 4 times shorter than the pulse (2 s/0.5 s).¹⁷

Summarizing, when selecting operational conditions for an ED system, the trade-off between energy consumption, capital investment (including membrane area and staging), and water recovery should be considered. PFPW being highly viscous and containing high concentrations of polymers does not behave like common brackish water; hence, literature guidelines for designing and operating a system to minimize the total costs of regular brackish water desalination¹⁸ might not be fully applicable and the costs and implications for PFPW desalination can be very different. For example, Thiel et al. estimated that, in practice, the minimum work necessary to desalinate high-salinity produced water could be up to 9 kWh/m³, nearly an order of magnitude higher than for seawater desalination.¹⁹

Operational conditions for an ED system can vary quite significantly, and the selection and design of an adequate ED configuration for a certain application require a thorough understanding of the relationships among energy consumption, capital costs, and water recovery. Furthermore, the possibility of using a pulsed electric field has not been explicitly considered in the reports available in the literature. Therefore, this study has two objectives: (1) to evaluate PFPW desalination at conditions close to the foreseen industrial application, specifically operating at high water recoveries, and at close-to-limiting current density, and (2) to use the collected data to relate performance in terms of energy consumption, capital costs, and water recovery and to identify strategies to cope with their trade-offs.

To achieve these objectives, the study is subdivided into three sections. In [Section 1](#), the water recovery was systematically increased while evaluating the effects of energy consumption and water transport. In [Section 2](#), the performance and fouling sensitivity of two ED stacks composed of different IEMs were evaluated. Finally, [Section 3](#) employs the results from the previous two to scrutinize the energy–membrane area–water recovery trade-offs and to discuss the feasibility of using PEF during the process.

2. MATERIALS AND METHODS

2.1. Preparation of Solutions and Chemicals. The feed solutions consisted of a mixed salt solution, referred to as brackish water (BW), and viscosifying polymer (BW+P). The BW solutions were prepared in demineralized water, according to the composition of water produced in the Marmul field (Oman), by adding the following salts: 53.3 mM NaCl, 15.6 mM NaHCO₃, 2.51 mM Na₂SO₄, 0.72 mM KCl, 0.65 mM CaCl₂, and 0.46 mM MgCl₂.¹⁵ The pH of the fresh solutions was 7.7, and their conductivity was 7.75 mS/cm. At these conditions, the viscosifying polymer is negatively charged, as explained in a previous publication.⁷

All BW+P solutions had a concentration of 0.5 g/L of partially hydrolyzed polyacrylamide (HPAM). This polymer concentration is within the range of water produced in real oil fields.²⁰ They were prepared by slowly pouring the polymer inside the BW solution under fast agitation, after which the mixture was left stirring at low speed overnight. Other typical components of polymer-flooding produced water would be crude oil and suspended solids, but their impact during electrodialysis experiments is much minor compared to that of HPAM.^{4,21}

The salts employed to prepare the solutions (NaCl, KCl, MgCl₂·6H₂O, CaCl₂·2H₂O, Na₂SO₄, and NaHCO₃) were of analytical grade, purchased from VWR (Belgium), and employed without further purification. The HPAM employed was Flopaam 3130S (*M_w* = 4.4–4.8 million Da and 30% hydrolyzed), kindly provided by SNF (France). NaOH and HCl solutions utilized for chemical cleaning were prepared from analytical-grade reagents purchased from VWR.

2.2. Electrodialysis Setup. Experiments were performed in ED stacks that have been previously described.⁷ Two configurations were used:

- FujiFilm (FF) stack. Contained seven FujiFilm type 10 AEMs, six cation-exchange membranes (CEMs) type 10, and two Neosepta CMX, which were placed at both ends of the stack as shielding membranes.

Table 1. Summary of ED Runs Performed during This Study

run/set	stack	V_D (L)	V_C (L)	stages	mode	i (A/m ²)	replicates ^a
1a	FujiFilm	5.0	5.0	1	continuous	40	3
1b	FujiFilm	5.0	3.0	1	continuous	40	1
1c	FujiFilm	5.0	2.0	1	continuous	40	1
1d	FujiFilm	5.0	1.0	1	continuous	40	1
1e	FujiFilm	5.0	0.5	1	continuous	40	3
2a	FujiFilm and Neosepta	4.0	0.4	1	continuous	40	set of 3 runs
2b	FujiFilm and Neosepta	4.0	0.4	1	PEF 1 s/0.5 s	40	set of 3 runs
2c	FujiFilm and Neosepta	4.0	0.4	1	PEF 1 s/0.5 s	60	set of 3 runs

^aThe “3” means that the experiment was performed by triplicate. “Set of 3” indicates that the set consisted of three batch experiments performed continuously one after the other.

- (ii) Neosepta stack. Consisted of seven Neosepta AMX membranes, six CMS CEMs, and two Neosepta CMX as shielding membranes.

The FujiFilm membranes were kindly provided by FujiFilm Manufacturing Europe B.V., while the Neosepta membranes were purchased from Eurodia (France). The working area of each membrane (104 cm²), spacer, gasket, and electrode were the same as previously reported. The spacers used were 450 μ m thick. A potentiostat/galvanostat Ivium-n-Stat (Ivium Technologies, Netherlands) controlled the electrical current at the predetermined values and measured the potential difference over the cell. The potential difference was measured using two reference Ag/AgCl gel electrodes (QM711X, QIS, Netherlands) placed at the inlet of each of the electrode compartments. A scheme of the setup is included as Figure S1 in the Supporting Information.

The diluate, concentrate, and electrode rinse solutions were pumped by three independent MasterFlex pumps. The electrode rinse solution consisted of 2.0 L of Na₂SO₄ 20 g/L. The conductivities of the diluate and concentrate were measured in line with two conductivity probes (Orion DuraProbe 4-electrode conductivity cell 013005MD) placed before the ED stack. The probes were connected to a transmitter box (Orion Versastar Pro), which corrected the measured values to the reference value at 25 °C. The pH of the solutions was measured with two pH probes (MemoSENS Endress+Hauser) connected to a transmitter box (P862, QIS). Two back-pressure valves (0.25 bar) were placed at the outlet of the electrolyte solution to guarantee the complete wetting of the electrodes.

2.3. Electrodialysis Runs. The electrodialysis experiments were run in batch mode until the design conductivity of 2.0 mS/cm was reached in the diluate stream. Most of them were run at a constant current of 40 A/m², which was found to be the limiting current density when desalinating a 2.0 mS/cm solution prepared by diluting the BW solution with demineralized water (see Figure S1). Diluate and concentrate feed solutions had the same composition. Both were pumped at 260 mL/min (linear velocity of 2.0 cm/s), while the electrolyte was circulated at 170 mL/min. The ED runs were performed at 23 \pm 1 °C in a controlled-temperature laboratory.

Two sets of experiments were performed during this study, summarized in Table 1, together with their main conditions. For the water recovery set (#1), the only variable was the ratio between the volumes of the diluate (V_D) and concentrate (V_C), which had different values depending on the volume of the concentrate, which was varied between 5.0 and 0.5 L. The volume of the diluate was kept constant, aiming to obtain

similar amounts of product, which is the main goal when desalinating water for polymer-flooding applications. The rest of the operational parameters, including the volume of the diluate (5.0 L) and current density (40 A/m²), were kept constant. This set was run only with the FujiFilm stack.

Before each ED run, the solutions were circulated through the cell for 10 min before starting the measurements. During the experiment, the applied current, stack voltage, and transported charges were recorded using the software provided by Ivium (IviumSoft). The samples were periodically taken. The final volumes of the solutions were measured with a graduated cylinder. Immediately after each ED run, the stack was cleaned-in-place by circulating a sequence of solutions for 10 min each. The schedule included HCl solution (pH = 2), NaCl solution (5.0 g/L), NaOH solution (pH = 12), NaCl solution (5.0 g/L), and a final rinse of at least 15 min with the BW solution.^{22,23}

2.4. ED for Comparing the Performance of Two Stacks through Three Sequential Runs. For the second part of the study, two different ED stacks were employed, one composed of FujiFilm membranes and another composed of Neosepta membranes (Section 2.2). Besides the type of membranes, both stacks were identical, containing the same number of cell pairs, type of spacers, etc. Each of the stacks was employed to desalinate three consecutive batches of 4.0 L of the BW+P solution, each “set of 3 runs” operated in a different mode. Three modes were tested: one in continuous and two in PEF mode run at different current densities, as described in Table 1. The PEF regime was determined after performing preliminary experiments, included in Section S3 in the Supporting Information. After each set of 3 runs was finished, the stack was cleaned-in-place, as explained in Section 2.3.

2.5. Analytical Methods. **2.5.1. Solution Analysis.** Diluate and concentrate samples were taken during the experiments. Their content of cations was analyzed with inductive-coupled plasma optical emission spectroscopy (ICP-OES, Optima 5300DV, Perkin Elmer) and that of anions with ion chromatography (761 Compact IC, Metrohm). Total carbon, inorganic carbon, and total organic carbon (TOC) were measured using a TOC analyzer (Shimadzu TOC-VCPH).

2.5.2. Water Recovery and Energy Calculations. The water recovery (WR) was calculated by dividing the final volume of the diluate ($V_{D,f}$) by the sum of the initial volumes of the diluate ($V_{D,i}$) and concentrate ($V_{C,i}$)

$$WR = \frac{V_{D,f}}{V_{D,i} + V_{C,i}} \times 100 \quad (1)$$

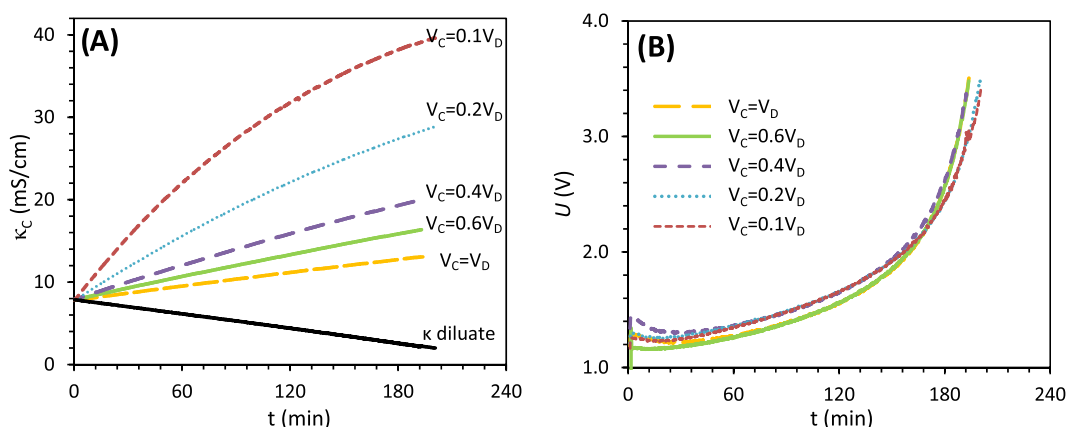


Figure 1. (A) Conductivity of the bulk concentrate solution (κ_c) measured during batch ED experiments desalinating 5.0 L of the diluate solution with different volumes of the concentrate (V_c) solution. (B) Electric potential (U) vs time (t) during the runs.

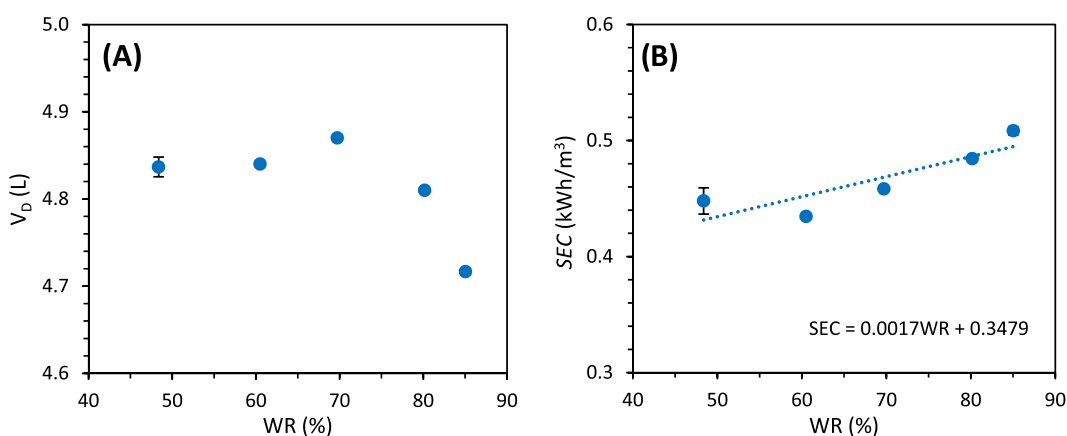


Figure 2. Diluate volume (A) and specific energy consumption (SEC) (B) vs water recovery (WR) calculated from the ED runs with varying concentrate volume. The error bars were calculated from experiments performed by triplicate.

The energy consumption (EC) was calculated by integrating the product of the current I (A) and the voltage U (V)²⁴

$$EC = \int I(t) \cdot U(t) dt \quad (2)$$

The specific energy consumption (SEC) was obtained from dividing the EC by the final volume of the diluate ($V_{D,f}$) in m³.

2.5.3. Osmotic and Electro-Osmotic Transport. The ionic composition of the streams, determined from the sample analysis, was used to calculate the flux of ions from the diluate to the concentrate stream and the concentrations in the bulk solutions. The total water flux was calculated from the volumes measured during the experiments. Then, the equations for osmotic and electro-osmotic water transport³ (respectively, eqs 3 and 4) were simultaneously solved to assign the amount of water transported as osmotic or electro-osmotically driven. In eq 3, the flux of water transported by osmosis J_{osm} (mol/m²/s) is directly related via the diffusion coefficient D_w (m²/s) to the driving force, which is the difference in molar concentration (mol/m³) between the diluate (c_d) and the concentrate (c_c). In the same equation, δ is the membrane thickness (m), Δm is the amount of water transported (mol), A is the membrane area (m²), and t is the time (s)

$$J_{osm} = D_w \frac{(c_c - c_d)}{\delta} = \frac{\Delta m}{A \cdot t} \quad (3)$$

As shown in eq 4, the water flux due to electro-osmosis (J_{eosm}) (mol/m/s) is proportional to the flux of positive and negative ions J_i (mol/m/s) and t_w , which is the average water transport number for a specific membrane pair (mol-H₂O/F)

$$J_{eosm} = t_w \sum_i J_i \quad (4)$$

The parameters D_w and t_w were simultaneously determined by employing a nonlinear solving method that would minimize the square of the differences between the concentrations measured and those estimated. The constraints given to the program were $0 < D_w < 1$ and $4 < t_w < 20$.

3. RESULTS AND DISCUSSION

3.1. Water Transport and Energy Consumption as Water Recovery Is Increased. The first objective of this work was to increase the water recovery (WR) of the process. The initial volume of the concentrate solution ($V_{C,i}$) was systematically decreased from 1.0 to 0.1 times the volume of the diluate ($V_{D,i}$) to achieve a higher water recovery. Since the rest of the parameters were maintained, including the volume and composition of the diluate solution, the amount of salts transferred from the diluate to concentrate solution was essentially the same. This implied that for smaller volumes of concentrate, the resulting salt concentration was higher, as indicated by the measured conductivities in the bulk solution, presented in Figure 1A. This had a small effect on the electric

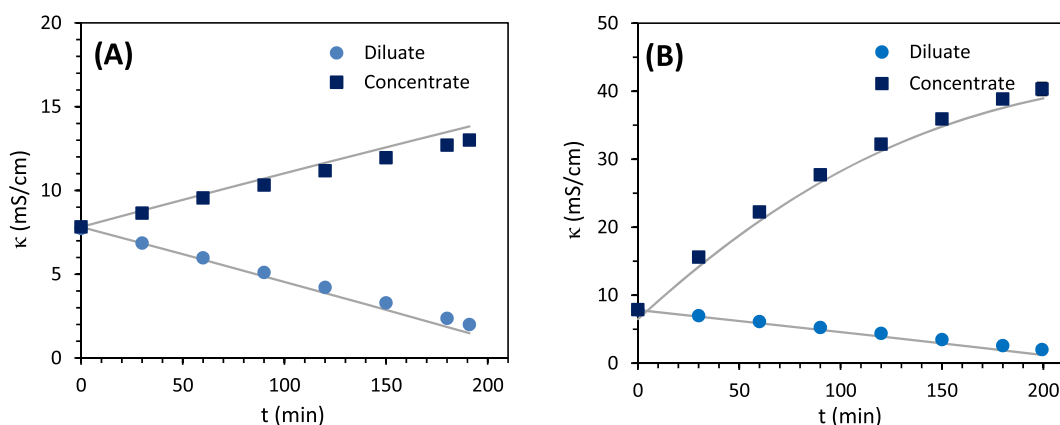


Figure 3. Average conductivities of the diluate and the concentrate streams vs time for experiments with 48% WR (A) and 85% WR (B). The modeled values consider 90% current efficiency, $t_w = 11$, and $D_w = 1.91 \times 10^{-9} \text{ m}^2/\text{s}$.

potential required to maintain the desalination at constant current, as presented in Figure 1B.

Another effect of increasing the water recovery was a higher amount of water transport, which can be inferred from differences in recovered diluate volumes (Figure 2A). Free water transport (osmosis) occurs due to the difference in osmotic pressure between the diluate and the concentrate streams, and the larger the difference is, the higher the water transport. The relation between the driving force and the flux of water transported by osmosis can be characterized by the water transfer or diffusion coefficient D_w (m^2/s).³ However, water is also transported in the hydration shell of the ions that migrate from the diluate to concentrate, commonly referred to as electro-osmosis. The water flux due to electro-osmosis is related to the flux of ions through the average water transport number for a specific membrane pair t_w ($\text{mol H}_2\text{O}/\text{F}$).²⁵ By employing the method described in our previous work,³ the values of t_w and D_w for the pair of FujiFilm type 10 membranes were, respectively, estimated as 11 mol $\text{H}_2\text{O}/\text{F}$ and $1.91 \times 10^{-9} \text{ m}^2/\text{s}$. Both values are higher than those previously determined for the membrane pair Neosepta CMX/AMX ($t_w = 8$ and $D_w = 2.0 \times 10^{-10} \text{ m}^2/\text{s}$),³ indicating that FujiFilm membranes allow higher osmotic and electro-osmotic transport. Figure 3 shows how the modeled conductivity values, based on ion migration and water transport, compare with the experimental data for the runs with the lowest and the highest WR. For the modeling, a current efficiency of 90%, defined as the total amount of electric charge transported by ions divided by the electric charge applied to the system, was assumed.³

Finally, when plotting the specific energy consumption (SEC, calculated via eq 2), as a function of WR (Figure 2B), it can be noticed that by increasing the WR from 48 to 85%, the SEC was also higher, from 0.43 to 0.50 kWh/ m^3 . This was caused by the combination of slightly higher electric potential required to transport the salts across the IEMs and the reduction in the volume of products due to water transport.

3.2. Comparison of an Aromatic (Neosepta) and an Aliphatic (FujiFilm) Stack in Different Operation Modes.

The second experimental part consisted of performing sets of three batch desalinations in series, without cleaning the ED stack in between, with the aim of comparing their performance after fouling has occurred. As shown in Figure 4, three different operational scenarios were tested using the Neosepta and FujiFilm stacks: (A) continuous ($40 \text{ A}/\text{m}^2$), (B) PEF mode (1 s/0.5 s) with $40 \text{ A}/\text{m}^2$ pulses ($\bar{i} = 26.7 \text{ A}/\text{m}^2$), and (C) PEF

mode (1 s/0.5 s) with $60 \text{ A}/\text{m}^2$ pulses ($\bar{i} = 40 \text{ A}/\text{m}^2$). There were considerable differences in the operative time and electric potential required to desalinate the three consecutive batches of PFPW depending on the stack and mode of operation. Among the several details that can be elaborated, our discussion will focus on three: time differences between runs, water transport, and energy consumption.

The time differences from run to run can be better appreciated in Figure 5A. Although the differences are small, it is curious to notice that while for the FujiFilm stack the second and third runs tended to be longer than the first one, the opposite occurred for the Neosepta stack. Based on our previous work,¹⁰ this could be an indication of some HPAM fouling the FujiFilm IEMs and reducing their permselectivity, which causes an increase in the transport of counterions and a decrease in efficiency, thus increasing the time of the run. In contrast, the duration of the experiments performed with the Neosepta stack was highly consistent from run to run, so apparently no changes in permselectivity occurred. The largest time difference for the Neosepta stack occurred between the first and second runs of the continuous experiments; this may be explained by the fact that the first run of the stack was done with new membranes, which were apparently still stabilizing during the first run.

Figure 5A also shows important differences in the run time between the continuous and PEF modes. The continuous mode (set 2a) and the PEF mode at $60 \text{ A}/\text{m}^2$ (set 2c) had the same average current density ($40 \text{ A}/\text{m}^2$), so their operational times were expected to be the same. Indeed, the operational times of the referred sets for both membranes only differed an average of 10%, a small difference that could be attributed to some back-diffusion during the pause times.⁷ For the PEF mode at $40 \text{ A}/\text{m}^2$ (set 2b), the expected run time would be 1.5 times that of the continuous mode because the system is not desalting for one-third of the operational time. This 1.5-fold increase of the operational time was observed for the Neosepta stack, but for the FujiFilm stack, the operational time doubled, much more than was expected. This was due to the higher water transport, as will be explained in the following paragraphs.

Water transport had also major consequences on the results presented in Figures 4 and 5. It did not only have implications in terms of reducing water recovery but also extended the operational time because it implies that the remaining salts are dissolved in a smaller volume, so more ions had to be

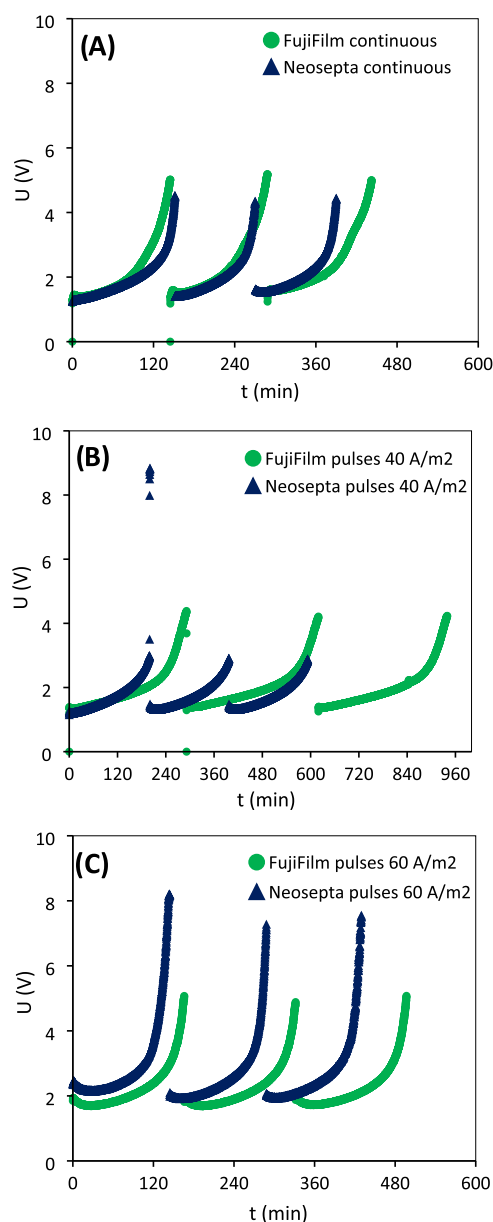


Figure 4. Electric potential (U) vs time during batch runs performed in sequence without cleaning-in-place. (A) Continuous operation at 40 A/m², (B) pulsed operation of 1 s/0.5 s, with 40 A/m² pulses, and (C) pulsed operation of 1 s/0.5 s, with 60 A/m² pulses.

transported to reach the desired quality in the diluate. Then, as shown in Figure 4A, when operated in continuous mode, the FujiFilm stack required roughly 50 more minutes over the 390 min used by the Neosepta stack to complete the three ED runs. Moreover, the average WR achieved by the FujiFilm stack was 83.4%, while for the Neosepta stack, it was 89.8% (Figure 5B). These results can be related to the differences between the electro-osmotic and diffusion coefficients for both membranes, presented in Section 3.1. On average, 440 mequiv of ions was transported from the diluate to concentrate during each of the runs, which implied an electro-osmotic transport of ~60 mL of water for the Neosepta stack and ~90 mL for the FujiFilm stack (considering $t_w = 8$ mol H₂O/F and $t_w = 11$ mol H₂O/F, respectively). For the Neosepta stack, practically all of the water was transported, meaning that water transport via diffusion did not play an important role, as expected from the

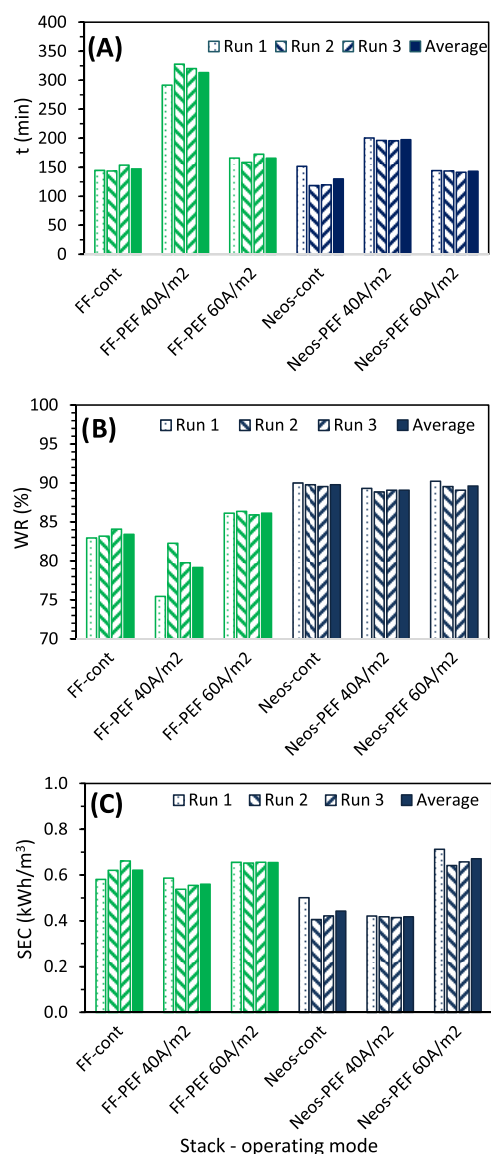


Figure 5. Running time (A), water recovery WR (B), and specific energy consumption SEC (C), obtained when operating the FujiFilm and Neosepta stacks in different modes to desalinate three batches of PFPW until reaching a conductivity of 2.0 mS/cm.

low osmotic diffusion coefficient ($D_w = 2.0 \times 10^{-10}$ m²/s). On the contrary, the osmotic diffusion coefficient calculated for the FujiFilm stack was 1 order of magnitude larger ($D_w = 1.9 \times 10^{-9}$ m²/s), and our measurements also indicated that most of the water transport (65%) can be attributed to osmosis.

Still addressing water transport, its effects were maximized during the pulsed operation at 40 A/m² (Figure 4B): while the total time required by the Neosepta stack was ~600 min, the operation with the FujiFilm stacks lasted more than 900 min. Similarly, the average duration of a run was under 200 min for Neosepta and 300 min for FujiFilm (Figure 5A). For both stacks, the transport of water through electro-osmosis should have been the same as calculated for the continuous mode (since a similar number of salt equivalents were transported), but the osmotic transport increased due to the extended operational time. By comparing the conductivity measurements vs time (Supporting Information, Figure S4), it can be deduced that during the runs with the FujiFilm stack, forward

salt transported during the pulse and backward water transported during the pause approached balancing values, which caused the extra operational time. However, these negative effects of elevated water transport in the FujiFilm stack were minimized by operating at 60 A/m² (Figures 4C and 5B). In that case, the average operative time per run with the FujiFilm stack was 165 min, only 22 min longer than for the Neosepta stack, and the water recovery was 3% higher than for the continuous runs (Figure 5B).

In terms of energy consumption, Figure 5C shows that when operated in continuous mode or in PEF with low current density pulses (40 A/m²), the Neosepta stack achieves the desired desalination with a lower SEC. However, the performance of the FujiFilm stack improves when operated at higher currents due to lower operative time (meaning lower water transport) and lower membrane resistance compared to the Neosepta membranes.¹⁰ Thus, when operated in PEF mode with 60 A/m² pulses, the SEC of the FujiFilm stack (0.65 kWh/m³) is slightly lower than that of Neosepta one (0.67 kWh/m³). Additional experiments performed in PEF with 100 A/m² pulses (\bar{i} = 66.7 A/m²) resulted in 1.24 kWh/m³ for the FujiFilm stack and 1.43 kWh/m³ for the Neosepta one (plots included in Figure S5). This confirmed the tendency of improved performance of the FujiFilm stack when higher current densities are employed.

3.3. Inter-Relative Analysis of Water Recovery, Energy Use, and Implemented Membrane Area. The current densities employed in the previous sections fall in the lower end of the recommended range to minimize costs for BW desalination.¹⁸ However, this disadvantage could be compensated by the savings when reusing the desalted water, especially since they also imply savings in polymers. Thus, we performed an economic analysis to identify if the current process design would be satisfactory enough to move onwards to the scaling up of the process. Table 2 includes the parameters and values employed for the calculations.

Table 2. Parameters Used for Cost Estimation

parameter	value
installed membrane cost	150, 250, 500 \$/m ²
apparent flux with current stack at 40 A/m ²	9.1 L/m ² h
annual utilization	8000 h
membrane lifetime ²⁶	6 years
energy consumption pumps and others	0.4 kWh/m ³
electricity cost	0.05 \$/kWh
amount of HPAM saved ^{3,27}	0.5 kg/m ³
price of HPAM ²⁸	1.0, 1.5, 2.5 \$/kg

The costs were calculated by adding up the installed membrane costs and the energy costs, both in \$/m³. As can be observed in Figure 6, three cases were evaluated, low, moderate, and high, depending on the price of the installed membrane area, which were assumed to be 100, 200, and 500 \$/m², respectively. These values were determined based on the prices of different commercial IEMs and are in agreement with the recent literature.²⁹ The energy cost was calculated by adding up the pumping cost (fixed at 0.4 kWh/m³) and the energy for desalination cost. The desalination costs and membrane costs were calculated simultaneously, from the data presented in Sections 3.1 and 3.2 of this study, as follows: a stack containing 0.146 m² of the total membrane area (7 cell pairs × 104 cm²) produced approximately 4.0 L of the diluate

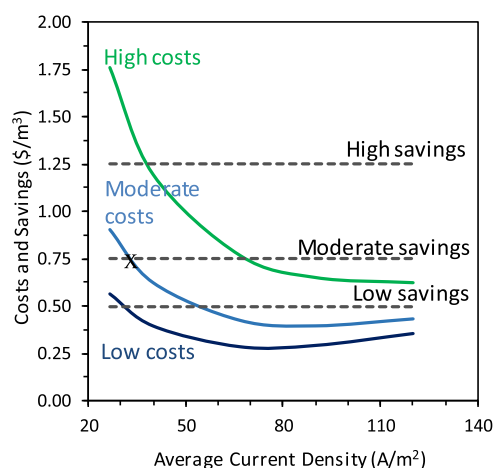


Figure 6. Estimation of costs and savings for polymer-flooding produced water desalination as a function of the average current density. Low, moderate, and high costs and saving scenarios are based on the information supplied in Table 2.

in 3 h of operation at an average current density of 40 A/m². Hence, for this current density, the apparent flux is 9.1 L/m²h. Assuming an annual utilization of 8000 h and a membrane lifetime of 6 years,²⁶ each square meter of the installed membrane has a total production capacity of 437 m³ of diluate, or inversely, 2.28×10^{-3} m² of the membrane area is needed per cubic meter of the product. Similar calculations were performed for other current densities, some evaluated during this work (26.7 and 66 A/m²), and some extrapolated (90 and 120 A/m²), resulting in energy costs ranging from 0.05 to 0.24 \$/m³ and membrane costs between 1.71 and 0.11 \$/m³. Thus, for most of the evaluated cases, the membrane cost dominates total costs, similar to previous calculations for brackish water desalination.¹⁸

On the other hand, the only savings considered were those from a reduced polymer consumption. The reason for this is that the polymer is relatively costly, and the saving of water use and discharge are highly case-dependent. In this generic assessment, these were not capitalized but could add case-specific benefits on top of those assessed here. From our previous research, it was found that by desalinating the PFPW, at least 0.5 kg/m³ of HPAM could be saved,³ an estimation supported by other studies.²⁷ For the calculations, three cases were evaluated, low, moderate, and high savings, depending on the price of the polymer HPAM (1.0, 1.5, and 2.5 \$/kg).

Finally, Figure 6 shows that when moderate costs and savings are considered, the break-even point (indicated with an X in the figure) occurs at a relatively low current density of 30 A/m². At low membrane costs, even low end in polymer savings offers a favorable business case at current densities of 35 A/m². Only when the membrane costs are in the high end, high polymer savings would be necessary to compensate for the operation at low current densities.

4. CONCLUSIONS

During this study, the use of aliphatic vs aromatic membranes and the application of pulsed electric field were experimentally tested to increase the water recovery and reduce the energy consumption during PFPW desalination. Water transport through the ion-exchange membranes tested showed significant differences. The high water permeability of aliphatic FujiFilm-10 IEMs affected both energy consumption and the

final water recovery of an electrodialysis-based process. However, it was also shown that most of the water transport could be attributed to the osmotic component, which becomes less significant when the ED was operated at higher current densities, so the performance of the stack containing aliphatic membranes equalized that of the stack containing the aromatic ones. Therefore, in terms of specific energy consumption, the Neosepta stack showed the best performance when operated in continuous or PEF mode with average current densities equal or under 40 A/m². Then, when operating at average current densities above 40 A/m², the FujiFilm stack outperforms the Neosepta one.

Regarding the application of pulsed electric field, comparisons made for the same average current density applied in PEF and in continuous mode showed higher specific energy consumption (SEC) for the Neosepta stack operated in PEF and practically no impact in the case of the FujiFilm stack. Although fouling might have formed after desalinating three consecutive batches, its effect on the overall performance of the stacks was minimal. In previous studies,^{7,10} membrane resistance measurements before and after the ED runs were performed to determine membrane damage due to irreversible fouling, but the changes observed were minimal.

The economic analysis demonstrated that the recovery of PFPW with ED at low current density offers a realistic business case with the potential to be further improved if higher current densities are achieved. This could be achieved either by applying the PEF mode or by employing stacks that allow operation with higher cross flow velocities and hence higher limiting current densities. Beyond savings in polymer use, additional, but case-specific economic and sustainability benefits can be achieved by the reuse of water, which can be a significant factor in fresh water-scarce areas where many oil and gas production sites are located.³⁰

■ ASSOCIATED CONTENT

Supporting Information

The Supporting Information is available free of charge at <https://pubs.acs.org/doi/10.1021/acs.iecr.0c02088>.

Scheme of the setup, plots of the determination of limiting current density at different flow rates, description and plots of preliminary experiments to find the optimal pause time during PEF with 1 s pulse, conductivity measurements during ED runs from Section 3.2, additional ED runs in the PEF mode with 100 A/m² pulses, and calculations for the economic analysis (PDF)

■ AUTHOR INFORMATION

Corresponding Authors

Paulina A. Sosa-Fernandez — Wetsus, European Centre of Excellence for Sustainable Water Technology, 8911 CC Leeuwarden, Netherlands; Department of Environmental Technology, Wageningen University, 6700 EV Wageningen, Netherlands; orcid.org/0000-0001-9939-1766; Email: p.a.sosafernandez@utwente.nl

Jan W. Post — Wetsus, European Centre of Excellence for Sustainable Water Technology, 8911 CC Leeuwarden, Netherlands; Email: jan.post@wetsus.nl

Authors

Apurva Karemore — Wetsus, European Centre of Excellence for Sustainable Water Technology, 8911 CC Leeuwarden, Netherlands

Harry Bruning — Department of Environmental Technology, Wageningen University, 6700 EV Wageningen, Netherlands

Huub H. M. Rijnaarts — Department of Environmental Technology, Wageningen University, 6700 EV Wageningen, Netherlands

Complete contact information is available at: <https://pubs.acs.org/doi/10.1021/acs.iecr.0c02088>

Author Contributions

The manuscript was written through the contributions of all authors. All authors have given approval to the final version of the manuscript.

Notes

The authors declare no competing financial interest.

■ ACKNOWLEDGMENTS

This work was performed in the cooperation framework of Wetsus, European Centre of Excellence for Sustainable Water Technology (www.wetsus.nl). Wetsus is co-funded by the Dutch Ministry of Economic Affairs and Ministry of Infrastructure and Environment, the European Union Regional Development Fund, the Province of Fryslân, and the Northern Netherlands Provinces. This research has received funding from the European Union's Horizon 2020 research and innovation program under the Marie Skłodowska-Curie Grant Agreement No. 665874. The authors are grateful to the participants of the research theme "Desalination" for their fruitful discussions and financial support.

■ ABBREVIATIONS

AEM	anion-exchange membrane
BW	brackish water
CEM	cation-exchange membrane
ED	electrodialysis
FF	FujiFilm
HPAM	partially hydrolyzed polyacrylamide
IEM	ion-exchange membrane
PEF	pulsed electric field
PFPW	polymer-flooding produced water
SEC	specific energy consumption
WR	water recovery

■ REFERENCES

- (1) Guolin, J.; Xiaoyu, W.; Chunjie, H. The Effect of Oilfield Polymer-Flooding Wastewater on Anion-Exchange Membrane Performance. *Desalination* **2008**, *220*, 386–393.
- (2) Jing, G.; Xing, L.; Li, S.; Han, C. Reclaiming Polymer-Flooding Produced Water for Beneficial Use: Salt Removal via Electrodialysis. *Desalin. Water Treat.* **2011**, *25*, 71–77.
- (3) Sosa-Fernandez, P. A.; Post, J. W.; Bruning, H.; Leermakers, F. A. M.; Rijnaarts, H. H. M. Electrodialysis-Based Desalination and Reuse of Sea and Brackish Polymer-Flooding Produced Water. *Desalination* **2018**, *447*, 120–132.
- (4) Sosa-Fernandez, P. A.; Miedema, S. J.; Bruning, H.; Leermakers, F. A. M.; Rijnaarts, H. H. M.; Post, J. W. Influence of Solution Composition on Fouling of Anion Exchange Membranes Desalinating Polymer-Flooding Produced Water. *J. Colloid Interface Sci.* **2019**, *557*, 381–394.

- (5) Guo, H.; Xiao, L.; Yu, S.; Yang, H.; Hu, J.; Liu, G.; Tang, Y. Analysis of Anion Exchange Membrane Fouling Mechanism Caused by Anion Polyacrylamide in Electrodialysis. *Desalination* **2014**, *346*, 46–53.
- (6) Mikhaylin, S.; Bazinet, L. Fouling on Ion-Exchange Membranes: Classification, Characterization and Strategies of Prevention and Control. *Adv. Colloid Interface Sci.* **2016**, *229*, 34–56.
- (7) Sosa-Fernandez, P. A.; Post, J. W.; Ramdhan, M. S.; Leermakers, F. A. M.; Bruning, H.; Rijnaarts, H. H. M. Improving the Performance of Polymer-Flooding Produced Water Electrodialysis through the Application of Pulsed Electric Field. *Desalination* **2020**, *484*, No. 114424.
- (8) Wang, T.; Yu, S.; Hou, L. Impacts of HPAM Molecular Weights on Desalination Performance of Ion Exchange Membranes and Fouling Mechanism. *Desalination* **2017**, *404*, 50–58.
- (9) Zuo, X.; Wang, L.; He, J.; Li, Z.; Yu, S. SEM-EDX Studies of SiO₂/PVDF Membranes Fouling in Electrodialysis of Polymer-Flooding Produced Wastewater: Diatomite, APAM and Crude Oil. *Desalination* **2014**, *347*, 43–51.
- (10) Sosa-Fernandez, P. A.; Post, J. W.; Nabaala, H. L.; Bruning, H.; Rijnaarts, H. H. Electrodialysis reversal and evaluation of different anion exchange membranes for the desalination of (waste)water produced after polymer-flooding, submitted for publication, 2020.
- (11) Turek, M.; Mitko, K.; Piotrowski, K.; Dydo, P.; Laskowska, E.; Jakóbi-Kolon, A. Prospects for High Water Recovery Membrane Desalination. *Desalination* **2017**, *401*, 180–189.
- (12) Strathmann, H. Ion-Exchange Membrane Processes in Water Treatment. In *Sustainability Science and Engineering*; Elsevier, 2010; Vol. 2, pp 141–199.
- (13) Valero, F.; Barceló, A.; Arbós, R. Electrodialysis Technology. Theory and Applications. In *Desalination, Trends and Technologies*; Schorr, M., Ed.; InTech Europe: Rijeka, 2011; pp 3–20.
- (14) Doornbusch, G. J.; Tedesco, M.; Post, J. W.; Borneman, Z.; Nijmeijer, K. Experimental Investigation of Multistage Electrodialysis for Seawater Desalination. *Desalination* **2019**, *464*, 105–114.
- (15) Al-Hashmi, A. R.; Divers, T.; Al-Maamari, R. S.; Favero, C.; Thomas, A. In *Improving Polymer Flooding Efficiency in Oman Oil Fields. Paper SPE-179834-MS*, SPE EOR Conference at Oil and Gas West Asia, Muscat, Oman, 21–23 March, 2016; p 18.
- (16) Ayrala, S. C.; Uehara-Nagamine, E.; Matzakos, A. N.; Chin, R. W.; Doe, P. H.; van den Hoek, P. J. In *A Designer Water Process for Offshore Low Salinity and Polymer Flooding Applications*, SPE Improved Oil Recovery Symposium, 2013.
- (17) Mikhaylin, S.; Nikonenko, V.; Pourcelly, G.; Bazinet, L. Intensification of Demineralization Process and Decrease in Scaling by Application of Pulsed Electric Field with Short Pulse/Pause Conditions. *J. Membr. Sci.* **2014**, *468*, 389–399.
- (18) Chehayeb, K. M.; Farhat, D. M.; Nayar, K. G.; Lienhard, J. H., V Optimal Design and Operation of Electrodialysis for Brackish-Water Desalination and for High-Salinity Brine Concentration. *Desalination* **2017**, *420*, 167–182.
- (19) Thiel, G. P.; Tow, E. W.; Banchik, L. D.; Chung, H. W.; Lienhard, J. H., V Energy Consumption in Desalinating Produced Water from Shale Oil and Gas Extraction. *Desalination* **2015**, *366*, 94–112.
- (20) Al Kalbani, H.; Mandhari, M. S.; Al-Hadhrani, H.; Philip, G.; Nesbit, J.; Gil, L.; Gaillard, N. In *Treating Back Produced Polymer to Enable Use of Conventional Water Treatment Technologies*, Society of Petroleum Engineers—SPE EOR Conference at Oil and Gas West Asia 2014: Driving Integrated and Innovative EOR, 2014; pp 617–629.
- (21) Guolin, J.; Lijie, X.; Yang, L.; Wenting, D.; Chunjie, H. Development of a Four-Grade and Four-Segment Electrodialysis Setup for Desalination of Polymer-Flooding Produced Water. *Desalination* **2010**, *264*, 214–219.
- (22) Guo, H.; You, F.; Yu, S.; Li, L.; Zhao, D. Mechanisms of Chemical Cleaning of Ion Exchange Membranes: A Case Study of Plant-Scale Electrodialysis for Oily Wastewater Treatment. *J. Membr. Sci.* **2015**, *496*, 310–317.
- (23) Xia, Q.; Guo, H.; Ye, Y.; Yu, S.; Li, L.; Li, Q.; Zhang, R. Study on the Fouling Mechanism and Cleaning Method in the Treatment of Polymer Flooding Produced Water with Ion Exchange Membranes. *RSC Adv.* **2018**, *8*, 29947–29957.
- (24) Ruiz, B.; Sistat, P.; Huguet, P.; Pourcelly, G.; Araya-Farias, M.; Bazinet, L. Application of Relaxation Periods during Electrodialysis of a Casein Solution: Impact on Anion-Exchange Membrane Fouling. *J. Membr. Sci.* **2007**, *287*, 41–50.
- (25) Galama, A. H.; Saakes, M.; Bruning, H.; Rijnaarts, H. H. M.; Post, J. W. Seawater Predesalination with Electrodialysis. *Desalination* **2014**, *342*, 61–69.
- (26) Strathmann, H.; Grabowski, A.; Eigenberger, G. Ion-Exchange Membranes in the Chemical Process Industry. *Ind. Eng. Chem. Res.* **2013**, *52*, 10364–10379.
- (27) Vermolen, E. C. M.; Pingo-Almada, M.; Wassing, B. M.; Ligthelm, D. J.; Masalmeh, S. K.; Mohammadi, H.; Jerauld, G. R.; Panchareon, M. In *Low-Salinity Polymer Flooding: Improving Polymer Flooding Technical Feasibility and Economics by Using Low-Salinity Make-up Brine*, The SPE Improved Oil Recovery Symposium, USA, 2014.
- (28) AlSofi, A. M.; Blunt, M. J. Polymer Flooding Design and Optimization under Economic Uncertainty. *J. Pet. Sci. Eng.* **2014**, *124*, 46–59.
- (29) Tufa, R. A.; Noviello, Y.; Di Profio, G.; Macedonio, F.; Ali, A.; Drioli, E.; Fontananova, E.; Bouzek, K.; Curcio, E. Integrated Membrane Distillation-Reverse Electrodialysis System for Energy-Efficient Seawater Desalination. *Appl. Energy* **2019**, *253*, No. 113551.
- (30) Nasiri, M.; Jafari, I.; Parniankhoy, B. Oil and Gas Produced Water Management: A Review of Treatment Technologies, Challenges, and Opportunities. *Chem. Eng. Commun.* **2017**, *204*, 990–1005.